Graphical Abstract:

Pentacyclic and hexacyclic cucurbitacins from *Elaeocarpus petiolatus*

Four undescribed cucurbitacins (petiolaticins A–D) along with four known cucurbitacins were isolated from *Elaeocarpus petiolatus*. Petiolaticin A showed cytotoxicity against selected human breast and colorectal cancer cell lines, while petiolaticin D showed inhibition of viral entry mediated by a highly pathogenic avian influenza HA protein.

Elaeocarpus petiolatus

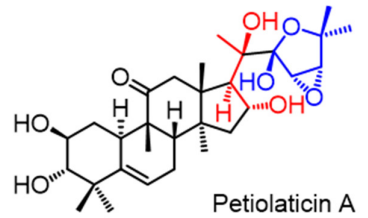

Petiolaticin A

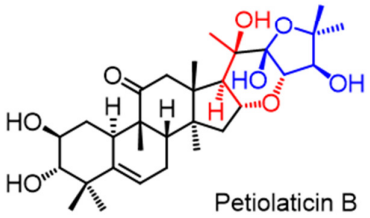

Petiolaticin B

Pentacyclic and hexacyclic cucurbitacins from *Elaeocarpus petiolatus*

Eun-Seon Cho[a], Premanand Krishnan[b], Hwei-San Loh[a], Janet M. Daly[c], Chee-Onn Leong[d,e], Chun-Wai Mai[e,f], Yun-Yee Low[g], Kien-Thai Yong[h], Kuan-Hon Lim[b,*]

[a] *School of Biosciences, University of Nottingham Malaysia, Jalan Broga, 43500 Semenyih, Selangor, Malaysia*

[b] *School of Pharmacy, University of Nottingham Malaysia, Jalan Broga, 43500 Semenyih, Selangor, Malaysia*

[c] *School of Veterinary Medicine and Science, University of Nottingham, Sutton Bonington, UK*

[d] *School of Pharmacy and* [e] *Centre for Cancer and Stem Cells Research, Institute for Research, Development and Innovation, International Medical University, 57000 Kuala Lumpur, Malaysia*

[f] *State Key Laboratory of Oncogenes and Related Genes, Renji-Med X Clinical Stem Cell Research Center, Department of Urology, Ren Ji Hospital, School of Medicine, Shanghai Jiao Tong University, Shanghai 200127, China*

[g] *Department of Chemistry, Faculty of Science, Universiti Malaya, 50603 Kuala Lumpur, Malaysia*

[h] *Institute of Biological Sciences, Faculty of Science, Universiti Malaya, 50603 Kuala Lumpur, Malaysia*

* Corresponding author.

E-mail address: KuanHon.Lim@nottingham.edu.my (K.-H. Lim).

ABSTRACT

Four undescribed cucurbitacins, designated as petiolaticins A–D, and four known cucurbitacins were isolated from the bark and leaves of *Elaeocarpus petiolatus* (Jack) Wall. Their chemical structures were elucidated based on detailed analyses of the NMR and MS data. The absolute configuration of petiolaticin A was also determined by X-ray diffraction analysis. Petiolaticin A represents a cucurbitacin derivative incorporating a 3,4-epoxyfuranyl-bearing side chain, while petiolaticin B possesses a furopyranyl unit fused to the tetracyclic cucurbitane core structure. Petiolaticins A, B and D were evaluated *in vitro* against a panel of human breast, pancreatic, and colorectal cancer cell lines. Petiolaticin A exhibited the greatest cytotoxicity against the MDA-MB-468, MDA-MB-231, MCF-7, and SW48 cell lines (IC_{50} 7.4, 9.2, 9.3, and 4.6 μM, respectively). Additionally, petiolaticin D, 16α,23α-epoxy-3β,20β-dihydroxy-10αH,23βH-cucurbit-5,24-dien-11-one, and 16α,23α-epoxy-3β,20β-dihydroxy-10αH,23βH-cucurbit-5,24-dien-11-one 3-*O*-β-$_D$-glucopyranoside were tested for their ability to inhibit cell entry of a pseudotyped virus bearing the hemagglutinin envelope protein of a highly pathogenic avian influenza virus. Petiolaticin D showed the highest inhibition (44.3%), followed by 16α,23α-epoxy-3β,20β-dihydroxy-10αH,23βH-cucurbit-5,24-dien-11-one (21.0%), and 16α,23α-epoxy-3β,20β-dihydroxy-10αH,23βH-cucurbit-5,24-dien-11-one 3-*O*-β-$_D$-glucopyranoside showed limited inhibition (9.0%). These preliminary biological assays have demonstrated that petiolaticins A and D possess anticancer and antiviral properties, respectively, which warrant for further investigations.

Keywords: *Elaeocarpus petiolatus*; Elaeocarpaceae; Cucurbitacins; Triterpenoids; X-ray crystallography; Cytotoxicity; viral entry inhibition

1. Introduction

Elaeocarpus is a genus of approximately 360 species that is distributed from the West Indian Ocean to the Pacific. *Elaeocarpus* is the largest of the 12 genera that make up the Elaeocarpaceae family (Tang and Phengklai, 2007). Despite being a relatively large genus, cucurbitacin-type triterpenoids (Cai et al., 2015; Chen et al., 2005) have

only been previously reported from six species, namely, *Elaeocarpus chinensis* (Pan et al., 2012), *Elaeocarpus dolichostylus* (Fang et al., 1984), *Elaeocarpus glabripetalus* (Zhang et al., 2010), *Elaeocarpus hainanensis* (Meng et al., 2008), *Elaeocarpus mastersii* (Ito et al., 2002), and *Elaeocarpus reticulatus* (Turner et al., 2020). In the Malay Peninsula, there are approximately 30 species of *Elaeocarpus*, some of which are traditionally used to treat headaches, fever, poultice sores, and as a general tonic (Aggarwal, 2001). Recently, we reported the first phytochemical investigation of an *E. tectorius* specimen collected from the west coast of Peninsular Malaysia (Ezeoke et al., 2018).

In our ongoing search for new and/or biologically active compounds from Malaysian flora (Chan et al., 2021; Krishnan et al, 2020), we detected the strong presence of cucurbitacins in the bark and leaf extracts of *Elaeocarpus petiolatus* (Jack) Wall. based on a preliminary screening. This plant is widely distributed in Malaysia and its leaves and roots are used locally to treat malaria and fever (Quattrocchi, 2012). However, there have been no studies on its phytochemical constituents. Furthermore, the ethanolic bark extract was reported to possess anti-inflammatory properties (Kwon et al., 2012). We now report the results of a phytochemical analysis of the leaves and bark of *E. petiolatus*, which has resulted in the discovery of four previously undescribed cucurbitacins, namely petiolaticins A–D (**1**–**4**), as well as four other known cucurbitacins **5**–**8** (Fig. 1). The *in vitro* cytotoxic effects of compounds **1**, **2**, and **4** against a panel of breast, pancreatic, and colorectal cancer cell lines, as well as viral entry inhibition potential of compounds **4**, **5**, and **6** against a highly pathogenic avian influenza haemagglutinin (HA)-based pseudotyped virus are also reported herein.

2. Results and discussion

From the bark EtOAc extract of *E. petiolatus*, petiolaticins A–C (**1**–**3**), 16*α*,23*α*-epoxy-3*β*,20*β*-dihydroxy-10*αH*,23*βH*-cucurbit-5,24-dien-11-one (**5**) (Meng et al., 2008), 16*α*,23*α*-epoxy-3*β*,20*β*-dihydroxy-10*αH*,23*βH*-cucurbit-5,24-dien-11-one 3-*O*-*β*-$_{D}$-glucopyranoside (**6**) (Muñoz et al., 2000), elaeocarpucin F (**7**) (Pan et al., 2012), and hexanocucurbitacin F (**8**) (Che et al., 1985) were isolated (Fig. 1). On the other hand, petiolaticin D (**4**) along with compounds **5**–**7** were obtained from the leaf EtOAc extract (Fig. 1).

Petiolaticin A (**1**) was initially obtained as a colorless oil with $[\alpha]_D$ +28 (*c* 0.9, $CHCl_3$). It was subsequently crystallized from $CHCl_3$/MeOH as block crystals (mp 180–182 °C). The IR spectrum showed absorption bands at 3408 and 1689 cm^{-1}, which were attributable to hydroxyl and carbonyl functions, respectively. HR-DART-MS measurements showed the $[M + H]^+$ peak at *m/z* 535.3252, which established the molecular formula of **1** as $C_{30}H_{46}O_8$. The ^1H NMR data of **1** (Table 1) showed eight methyl singlets at δ_H 0.94 (× 2), 1.08, 1.19, 1.27, 1.34, 1.39, and 1.50, an olefinic doublet at δ_H 5.73 (*J* = 5.8 Hz), a pair of AB doublets due to a ketomethylene group at δ_H 2.65 and 3.11 (*J* = 14.6 Hz), and five oxymethine resonances at δ_H 2.97, 3.47, 3.57, 3.84, and 4.60. The ^{13}C NMR data of **1** (Table 1) showed a total of 30 resonances, comprising eight methyl, four methylene, nine methine, and nine quaternary carbons. The observed carbon resonance at δ_C 213.7 indicated the presence of a ketone function, while the resonances at δ_C 119.2 and 140.6 were attributed to a trisubstituted double bond. Based on the HSQC data, the resonances at δ_C 59.6, 59.7, 71.0, 71.2, and 80.9 were assigned to five oxymethines, while the resonances at δ_C 77.4, 81.2, and 106.3 were assigned to two oxygenated tertiary carbons and a dioxygenated secondary carbon (hemiketal), respectively. The ^1H and ^{13}C NMR data of **1** showed a general resemblance to those of cucurbitacin F (**9**) (Kim et al., 1997), except for resonances due to C-22, C-23, C-24, and C-25 (part of the side chain located at C-17). The resonances due to the C-22 ketone and C-23–C-24 double bond in **9** were replaced with those due to the dioxygenated secondary carbon (δ_C 106.3) and epoxy function (δ_C 59.6, δ_H 3.84; δ_C 59.7 and δ_H 3.47) in **1**. The presence of the hemiketal furanyl moiety (C-22–C-23–C-24–C-25) containing an epoxy function in **1** was inferred by the key three-bond correlations observed from H-23 to C-25; from H-17, H-21 and H-24 to C-22; and from H-26 and H-27 to C-24 in the HMBC spectrum (Fig. 2). The planar structure proposed for **1** was completely consistent with the HMBC data (Fig. 2).

On the basis of the NOESY data (Fig. 3), the configurations at all chiral centers in **1**, except for those in the furanyl side chain (including C-20), were determined to be identical to those in **9**. The NOEs observed for H-8/CH_3-18, H-8/CH_3-19, and H-16/H-18 required H-8, H-16, CH_3-18, and CH_3-19 to be β-oriented (16-OH was α-oriented). On the other hand, the NOEs observed for H-10/CH_3-30 and H-17/CH_3-30 required H-10, H-17, and CH_3-30 to be α-oriented (the C-17–C-20 bond was β-oriented). In addition, the NOEs observed for H-2/CH_3-28 and H-3/CH_3-29 deduced that 2-OH and 3-

OH were β- and α-oriented, respectively. However, the stereochemistry in the furanyl side chain relative to the fused tetracyclic core structure could not be established with certainty based on the NOESY data due to free rotation about the C-17–C-20 bond. Fortunately, since suitable crystals of **1** were obtained, X-ray diffraction analysis using Cu Kα radiation was performed (Fig. 4), which not only confirmed the proposed planar structure, but also established the absolute configurations at all stereocenters in **1** as 2*S*,3*S*,8*S*,9*R*,10*R*,13*R*,14*S*,16*R*,17*R*,20*R*,22*R*,23*S*,24*R*.

Petiolaticin B (**2**) was obtained as a light yellowish oil with $[\alpha]_D$ +48 (*c* 0.4, $CHCl_3$). The IR spectrum showed absorption bands similar to those of **1**, i.e., OH (3406 cm^{-1}) and carbonyl (1688 cm^{-1}). The HR-DART-MS showed a significant peak at *m/z* 499.3054, which was analyzed for $[C_{30}H_{43}O_6]^+$ and corresponded to $[M + H - 2H_2O]^+$. The molecular formula of **2** was therefore determined to be $C_{30}H_{46}O_8$. The ^1H and ^{13}C NMR data (Table 1) of **2** showed a general resemblance to those of **1**, except for resonances associated with the furanyl side chain present in **1**. Most notably, the epoxy carbon resonances at δ_C 59.6 (δ_H 3.84, d) and δ_C 59.7 (δ_H 3.47, d) in **1** have been replaced by signals at δ_C 86.9 (δ_H 4.04, s) and δ_C 80.4 (δ_H 3.82), respectively, in **2**. The substantial downfield shift observed for these resonances suggested that the C-23–C-24 epoxy function in **1** was replaced with a 1,2-ethynedioxy fragment in **2**. Other notable ^{13}C NMR shift differences between **1** and **2** ($|\Delta\delta_C| > 3$ ppm) were observed for C-16, C-17, C-20, C-21, C-25, and C-27. These observations indicated that the structural differences between **1** and **2** were confined to the C-22–C-23–C-24–C-25 fragment and the C-16 hydroxyl group. The COSY and HMBC data of **2** confirmed that the fused tetracyclic core structure in **1** is also present in **2** (Fig. 2). Additionally, the correlations observed in the HMBC spectrum from H-16 to C-23; and from H-23 to C-16 suggested that a fifth fused ring was present in **2**, i.e., C-16 and C-23 were connected via an ether bridge to form a pyranyl ring. This suggestion was consistent with the observation that the C-23–C-24 epoxide carbons in **1** (δ_C 59.6 and 59.7) were replaced by the 1,2-ethynedioxy carbons (δ_C 86.9 and 80.4, respectively) in **2**. The presence of the pyranyl moiety in **2** was also supported by other correlations observed in the HMBC spectrum, i.e., from H-16 to C-20; from H-17 to C-22; from H-21 to C-17, C-20, and C-22; and from H-23 to C-22. As a result, the furanyl side chain in **1** was inferred to be the sixth fused ring in **2** based on the correlations observed in the HMBC spectrum from H-23 to

C-22, C-24, and C-25; from H-24 to C-22, C-23, C-25, and C-27; and from H-27 to C-24 and C-26.

The stereochemistry of the furopyranyl unit in **2** could be inferred based on analysis of the NOESY data (Fig. 3). The NOEs observed for H-16/H-18 and H-16/H-23 required H-16 and H-23 to be β-oriented (16*R*,23*S*), while the NOEs observed for H-17/CH_3-30 and H-17/CH_3-21 required H-17 and CH_3-21 to be α-oriented (20-OH was β-oriented) (17*R*,20*R*). Consequently, the NOE observed for H-17/CH_3-27 was only possible when the furopyranyl ring junction is *cis*-fused, thus requiring 22-OH to be β-oriented (22*R*). Lastly, the NOEs observed for H-24/CH_3-26 and H-24/CH_3-27 suggested that H-24 was α-oriented (24-OH was β-oriented) (24*S*), which is consistent with the lack of NOE between H-23 and H-24, indicating that they are not oriented on the same face. The relative configuration deduced for the furopyranyl unit in **2** was also consistent with the presence of H-23 and H-24 as slightly broad singlets in the ^{1}H NMR spectrum, indicating that they were only weakly coupled. Based on the energy-minimized models (MM2, Chem3D version 20.1) of **2** (16*R*,17*R*,20*R*,22*R*,23*S*,24*S*), the torsion angle between H-23 and H-24 was shown to be 84°, which corresponds to a small coupling constant value of ~1 Hz (Haasnoot et al., 1980; Donders et al., 1989). Therefore, the relative configurations at all stereocenters in **2** were determined as 2*S*,3*S*,8*S*,9*R*,10*R*,13*R*,14*S*,16*R*,17*R*,20*R*,22*R*,23*S*,24*S*.

Petiolaticin C (**3**) was obtained as a colorless oil with $[\alpha]_D$ +57 (*c* 0.3, $CHCl_3$). The IR spectrum showed bands due to OH (3447 cm^{-1}) and carbonyl (1688 cm^{-1}) functions. The HR-DART-MS measurements determined its molecular formula as $C_{30}H_{46}O_5$ based on the $[M + H - H_2O]^+$ peak at *m/z* 469.3327. The ^{1}H NMR spectrum of **3** (Table 2) revealed the presence of eight methyl singlets at δ_H 0.89, 0.91, 1.10, 1.17, 1.27, 1.31, 1.69 and 1.72, a pair of AB doublets due to a ketomethylene group at δ_H 2.44 and 2.99 (J = 14.7 Hz), and four oxymethine resonances at δ_H 3.26, 3.47, 4.37, and 4.54. The ^{13}C NMR spectrum of **3** (Table 2) showed a total of 30 resonances, comprising eight methyl, six methylene, eight methine, and eight quaternary carbons. The resonance observed at δ_C 212.8 indicated the presence of a ketone group, while those at δ_C 125.0 and 136.4 were due to a trisubstituted double bond. Along with the HSQC data, the resonances at δ_C 52.2, 72.9, 75.9, and 77.8 were attributed to four oxymethines, while the resonance at δ_C 72.2 and 65.4 to two oxygenated tertiary carbons. The ^{1}H and ^{13}C NMR data of **3** showed a general resemblance to those of 16α,23α-epoxy-3β,20β-

dihydroxy-10αH,23βH-cucurbit-5,24-dien-11-one (**5**), a known cucurbitacin first isolated from *Elaeocarpus hainanensis* (Meng et al., 2008), which was also obtained in the present study. Comparison of the NMR data of **3** with those of **5** showed several distinct differences, i.e., the olefinic resonances at δ_C 142 and δ_C 120 (δ_H 5.62) due to C-5 and C-6 in **5**, were replaced by resonances at δ_C 65.4 and δ_C 52.2 (δ_H 3.26) in **3**. These observations suggested that the C-5–C-6 trisubstituted double bond in **5** has been replaced with an epoxy function in **3**. This change was also reflected in the carbon shifts of CH_3-28 and CH_3-29 for both **3** and **5** (Meng et al., 2008), which were found to differ quite significantly, i.e., δ_C 24.7 and 20.4 in **3** vs δ_C 27.1 and 25.3 in **5**, respectively. The planar structure of **3** is entirely consistent with the COSY and HMBC data (Fig. 2). On the basis of the NOESY data (Fig. 3), the configurations at all stereocentres in **3**, except for the epoxy-containing C-5 and C-6, were determined to be identical to those in **5**. In addition, the NOEs observed for H-6/CH_3-29, H-6/H-7α, H-7β/CH_3-19, H-10/CH_3-28, and H-10/CH_3-30 revealed that the epoxy group was β-oriented (Kubo et al., 1996). Therefore, compound **3** was determined as the 5β,6β-epoxy derivative of **5**.

Petiolaticin D (**4**) was obtained as a white amorphous powder with $[\alpha]_D$ +79 (*c* 1.0, $CHCl_3$). The IR spectrum indicated the presence of OH (3414 cm^{-1}) and carbonyl (1683 cm^{-1}) functions. The HR-DART-MS measurements determined its molecular formula as $C_{38}H_{58}O_{10}$ based on the $[M + H]^+$ peak at *m/z* 675.4074. The ^1H and ^{13}C NMR data of **4** (Table 2) are generally similar to those of 16α,23α-epoxy-3β,20β-dihydroxy-10αH,23βH-cucurbit-5,24-dien-11-one 3-*O*-β-$_D$-glucopyranoside (**6**), except for the presence of an additional acetyl group in **4** (δ_H 2.09; δ_C 20.9 and 171.6). Compound **6** was previously identified from *Kageneckia oblonga* (Muñoz et al., 2000) and was obtained in the present study as the most abundant compound. The presence of the acetate group at C-6' in **4** was deduced based on the three-bond correlation observed from H-6' to C-7' in the HMBC spectrum (Fig. 2). This is also consistent with H-6' of **4** (δ_H 4.30) being significantly more deshielded compared to that of **6** (δ_H 3.38 and 3.65) (Muñoz et al., 2000). Finally, the successful conversion of **6** to **4** via selective acetylation of the primary alcohol group with acetic anhydride/pyridine at low temperatures confirmed that compound **4** is the 6'-*O*-acetyl derivative of **6**.

A plausible pathway to **1** and **2** starting from cucurbitacin F (**9**) is presented in (Fig. 5). A nucleophilic addition by 25-OH onto the C-22 ketone in **9** gives the 2,5-dihydrofuran intermediate (**10**). Oxidation of the 23,24-double bond in **10** then yields the

α- and β-epoxide intermediates, with the former corresponding to compound **1**. Finally, epoxide ring-opening following nucleophilic attack by 16-OH onto C-23 in the β-epoxide intermediate gives compound **2** (Hüttel et al., 2014; Little, et al., 2020).

Compounds **1**, **2**, and **4** were evaluated *in vitro* against a panel of human breast, pancreatic and colorectal cancer cell lines, as well as a non-tumorigenic human breast epithelial cell line, and their IC_{50} values are shown in Table 3. Between the breast and pancreatic cancer cell lines tested, compounds **1**, **2**, and **4** exhibited higher toxicity against the former, with compound **1** recorded the lowest IC_{50} values for MDA-MB-468, MDA-MB-231, and MCF-7 (IC_{50} 7.4, 9.2, and 9.3 μM, respectively). Both MDA-MB-468, MDA-MB-231 are triple negative breast cancer cell lines associated with a poor prognosis. Compound **1** was also evaluated on three colorectal cancer cell lines, showing selectivity against SW48 (IC_{50} 4.6 μM). Notably, compounds **1**, **2**, and **4** did not show significant toxicity against the non-tumorigenic breast epithelial cells (MCF-10A) (IC_{50} > 30 μM). Compounds **5**–**8** were previously reported to show no obvious cytotoxicity *in vitro* (Che et al., 1985; Meng et al., 2008; Muñoz et al., 2000; Pan et al., 2012). It was also postulated that the presence of the 16α,23α-epoxy linkage (which is present in **2**–**7**) is detrimental for cytotoxic activity (Meng et al., 2008; Muñoz et al., 2000). This postulation is somewhat consistent with compound **1** broadly showing better cytotoxic effects against the four breast cancer cell lines tested when compared to **2** and **4**.

Triterpenoids have recently been reported to exhibit inhibitory activities against influenza virus, human immunodeficiency virus, and hepatitis C virus (Si et al., 2018; Ye et al., 2020). The influenza virus hemagglutinin (HA) protein plays critical roles in the early stage of virus infection, including the adsorption of virus particles to the cell surface receptors and membrane fusion. Therefore, the HA protein has been widely regarded as a potential target for the development of anti-influenza drugs. Triterpenoids have been shown by Si et al. (2018) and Ye et al. (2020) to inhibit the entry of influenza A viruses by interacting with viral fusion proteins including HA. Therefore, in the current study, compounds **4**, **5**, and **6** were evaluated using an influenza HA pseudotyped virus in a viral entry inhibition assay. Without the compound (virus-only control), the pseudotyped virus was able to effectively enter the MDCK cells, resulting in the highest relative light units (RLU) (Fig. 6a). As shown in Fig. 6b, the greatest reduction in viral entry was seen with compound **4** (44.3% ± 6.4), followed by compound **5** (21.0% ± 9.0). Compound **6**, on the other hand, was unable to effectively

inhibit viral entry (9.0% ± 6.3). Further studies are required to determine the antiviral potential of compounds **4** and **5** against influenza A virus and other viruses, as well as to confirm their mechanism of action.

3. Conclusions

In this study, four previously undescribed cucurbitacin-type triterpenoids (**1**–**4**) along with four known compounds (**5**–**8**) were obtained and identified from the bark and leaves of *E. petiolatus*. Notably, petiolaticin A (**1**) represents a cucurbitacin-type triterpenoid incorporating a rare 3,4-epoxyfuranyl moiety, while petiolaticin B (**2**) possesses a furopyranyl unit fused to the tetracyclic cucurbitane core structure. Meanwhile, *in vitro* biological studies have shown that selected cucurbitacins possess anticancer and antiviral properties. Among the compounds tested, petiolaticin A (**1**) exhibited the greatest cytotoxicity against the MDA-MB-468, MDA-MB-231, MCF-7, and SW48 cell lines, while petiolactin D (**4**) demonstrated the greatest inhibition of cell entry mediated by a highly pathogenic avian influenza HA protein.

4. Experimental

4.1. General experimental procedures

Melting points of crystals were recorded on a Stuart SMP10 digital melting point apparatus and were uncorrected. Optical rotations were measured with a JASCO P-1020 digital polarimeter. UV spectra were performed on a PerkinElmer Lamda 35 UV/vis spectrophotometer, while IR spectra were obtained on a PerkinElmer Spectrum RX1 FT-IR spectrometer. 1D and 2D NMR spectra were obtained in $CDCl_3$ using TMS as an internal standard on a Bruker Avance III 600 MHz spectrometer. HRMS data were measured on a JEOL Accu TOF-DART mass spectrometer.

4.2. Plant material

The bark and leaves of *Elaeocarpus petiolatus* (Jack) Wall. (Elaeocarpaceae) were collected in August 2013 from Kajang (GPS 2° 57′39″N, 101° 48′30″E), Selangor, Malaysia, and the plant was identified by K.T. Yong (Institute of Biological Sciences, University of Malaya). A voucher specimen (KLU48271) has been deposited at the Herbarium, University of Malaya.

318

319 *4.3. Extraction and isolation*

320 The air-dried and ground bark (1.42 Kg) of *E. petiolatus* was extracted with
321 EtOAc (3 × 4 L). The extracts were concentrated to dryness under vacuum and
322 subsequently suspended in MeOH-water (4:1, 1 L). The suspension was extracted with
323 hexane (3 × 1 L), followed by $CHCl_3$ (5 × 1 L). The $CHCl_3$ fractions were combined
324 and concentrated to dryness under vacuum to afford 16.8 g of crude fraction. The $CHCl_3$
325 crude fraction was separated by vacuum liquid chromatography (silica gel 60; EtOAc–*n*-
326 hexane, EtOAc, and EtOAc–MeOH) to afford eleven fractions (EPB1–EPB11). Fraction
327 EPB3 (770 mg) was re-chromatographed using centrifugal preparative thin layer
328 chromatography (Chromatotron, silica gel 60, $CHCl_3$–MeOH 1:0 → 100:1) to give **3** (18
329 mg). Fraction EPB4 (1.2 g) was re-chromatographed using vacuum column
330 chromatography ($CHCl_3$–MeOH) to yield nine sub-fractions (EPB4/1– EPB4/9). Further
331 fractionation of EPB4/4 using centrifugal preparative thin layer chromatography
332 (Chromatotron, silica gel 60, Et_2O–*n*-hexane 4:1 → 1:0) gave **2** (15 mg), **5** (120 mg),
333 and **7** (5 mg). Fraction EPB5 (1.2 g) was re-chromatographed using centrifugal
334 preparative thin layer chromatography (Chromatotron, silica gel 60, $CHCl_3$–MeOH
335 100:1 → 20:1) to give **1** (24 mg) and hexanocucurbitacin F (**8**) (Che et al., 1985) (94
336 mg). Fractionation of EPB6 (5.4 g) using vacuum liquid chromatography
337 (Chromatotron, silica gel 60, EtOAc–MeOH 50:1 → 10:1), followed by further
338 purification by centrifugal preparative thin layer chromatography (Chromatotron, silica
339 gel 60, $CHCl_3$–MeOH 100:1 → 10:1) gave **6** (1.2 g).

340 The air-dried and ground leaves (619 g) of *E. petiolatus* were extracted with
341 EtOAc (3 × 3 L). The EtOAc extracts were concentrated to dryness under vacuum to
342 afford 43 g of crude extract. A portion of the EtOAc crude extract (12.8 g) was
343 fractionated by vacuum column chromatography with gradient elution (silica gel 60,
344 EtOAc–*n*-hexane, EtOAc, and EtOAc–MeOH) to afford eight fractions (EPL1–EPL8).
345 Fraction EPL5 (1.9 g) was re-chromatographed using vacuum column chromatography
346 ($CHCl_3$–MeOH) to yield eight sub-fractions (EPL5/1–EPL5/8). Further fractionation of
347 EPL5/6 using centrifugal preparative thin layer chromatography (Chromatotron, silica
348 gel 60, $CHCl_3$–MeOH 1:0 → 20:1) gave **5** (826 mg). Fraction EPL6 (225 mg) was
349 fractionated using centrifugal preparative thin layer chromatography (Chromatotron,
350 silica gel 60, Et_2O–*n*-hexane 1:1 → Et_2O–MeOH 100:1) to give **7** (20 mg). Fraction
351 EPL7 (1.18 g) was re-chromatographed using vacuum column chromatography ($CHCl_3$–

MeOH) to yield six sub-fractions (EPL7/1–EPL7/6). Further fractionation of EPL7/5 using centrifugal preparative thin layer chromatography (Chromatotron, silica gel 60, $CHCl_3$–MeOH 100:1 → 20:1) gave **4** (70 mg). Fraction EPL8 (964 mg) was fractionated using centrifugal preparative thin layer chromatography (Chromatotron, silica gel 60, EtOAc–MeOH 50:1 → 10:1) to give **6** (156 mg).

*4.3.1. Petiolaticin A (**1**)*

Colorless block crystals ($CHCl_3$/MeOH); mp 180–182 °C; $[\alpha]_D$ +28 (*c* 0.9, $CHCl_3$); UV (MeCN) λ_{max} (log ε) 196 (3.91), 231 (2.95) nm; IR ν_{max} 3408, 1689 cm^{-1}; ^1H NMR and ^{13}C NMR data, see Table 1; HR-DART-MS *m/z* 535.3252 $[M + H]^+$ (calcd for $C_{30}H_{47}O_8$, 535.3265).

*4.3.2. Petiolaticin B (**2**)*

Light yellowish oil; $[\alpha]_D$ +48 (*c* 0.4, $CHCl_3$); UV (MeCN) λ_{max} (log ε) 194 (3.77), 239 (2.98) nm; IR ν_{max} 3406, 1688 cm^{-1}; ^1H NMR and ^{13}C NMR data, see Table 1; HR-DART-MS *m/z* 499.3054 $[M + H - 2H_2O]^+$ (calcd for $C_{30}H_{43}O_6$, 499.3054).

*4.3.3. Petiolaticin C (**3**)*

Light yellowish oil; $[\alpha]_D$ +57 (*c* 0.3, $CHCl_3$); UV (MeCN) λ_{max} (log ε) 195 (3.90), 233 (2.99) nm; IR ν_{max} 3447, 1688 cm^{-1}; ^1H NMR and ^{13}C NMR data, see Table 2; HR-DART-MS *m/z* 469.3327 $[M + H - H_2O]^+$ (calcd for $C_{30}H_{47}O_5$, 469.3312).

*4.3.4. Petiolaticin D (**4**)*

White amorphous powder; $[\alpha]_D$ +79 (*c* 1.0, $CHCl_3$); UV (MeCN) λ_{max} (log ε) 194 (3.74), 266 (3.37) nm; IR ν_{max} 3414, 1683 cm^{-1}; ^1H NMR and ^{13}C NMR data, see Table 2; HR-DART-MS *m/z* 675.4074 $[M + H]^+$ (calcd for $C_{38}H_{59}O_{10}$, 675.4103).

*4.4. Acetylation of **6** to **4***

To a solution of **6** (20 mg, 0.03 mmol) in THF (2 mL) was added acetic anhydride (0.06 mmol) and pyridine (0.03 mmol). The mixture was kept in the dark at –20 °C for 72 h. The solvent was removed under reduced pressure and the resultant residue was chromatographed (Chromatotron, silica gel, $CHCl_3$–MeOH) to afford **4** (7.8 mg, 0.012 mmol, 40% yield).

385

386 *4.5. X-ray crystallography analysis of petiolaticin A (**1**)*

387 X-ray diffraction analysis was carried out on a Rigaku Oxford (formerly Agilent
388 Technologies) SuperNova Dual diffractometer with Cu Kα (λ = 1.54178 Å) radiation at
389 155 K. The structures were solved by direct methods (SHELXS-2014) and refined with
390 full-matrix least-squares on F^2 (SHELXL-2014). All non-hydrogen atoms were refined
391 anisotropically, and all hydrogen atoms were placed in idealized positions and refined as
392 riding atoms with the relative isotropic parameters. Crystallographic data for compound
393 **1** have been deposited with the Cambridge Crystallographic Data Centre. Copies of the
394 data can be obtained, free of charge, on application to the Director, CCDC, 12 Union
395 Road, Cambridge CB2 1EZ, UK (fax: +44 (0)1223-336033, or e-mail:
396 deposit@ccdc.cam.ac.uk).

397 Crystallographic data of **1**: Light yellowish block crystals ($CHCl_3$/MeOH/H_2O),
398 mp 180–182 °C, 2($C_{30}H_{46}O_8$).2(CH_3OH).H_2O, *M*r = 1151.43, monoclinic, space group
399 C_2, a = 30.0782(5) Å, b = 8.53996(13) Å, c = 11.86480(17) Å, β = 102.2829 (13)°, V =
400 2977.91(8) Å^3, Z = 2, D_{calcd} = 1.284 gcm^{-3}, crystal size 0.5 x 0.3 x 0.04 mm^3, F(000) =
401 1252, Cu Kα radiation (λ = 1.54178 Å), T = 155(2) K. The final R_1 value is 0.0310 (wR_2
402 = 0.0869) for 5851 reflections [$I>2\sigma(I)$]. The absolute configuration of compound **1** was
403 determined on the basis of Flack parameter [x = 0.03(0.07)] and corroborated by use of
404 the Hooft parameter [y = 0.05(0.03)]. CCDC number 2089714.

405

406 *4.6. Cell lines and cell culture conditions*

407 A panel of human breast (MDA-MB-468, MDA-MB-231, MCF-7, and SKBR3),
408 pancreatic (AsPC-1, BxPC-3, and SW1990), colorectal (SW48, Caco2, and HCT116)
409 cancer cell lines and non-tumorigenic MCF-10A breast epithelial cell line, purchased
410 from the American Type Culture Collection (ATCC, USA), were used for the evaluation
411 of luminescent cell viability assay. All cancer cells were maintained in RPMI 1640
412 medium supplemented with 10% fetal bovine serum (FBS), 100 IU/mL penicillin, and
413 100 μg/mL streptomycin (Sigma-Aldrich, St. Louis, MO, USA), while MCF-10A cells
414 were cultured in Dulbecco's Modified Eagle Medium/Nutrient Mixture F-12 (DMEM/F-
415 12) added with 5% horse serum, 20 ng/mL epidermal growth factor, 0.5 μg/mL
416 hydrocortisone, 10 μg/mL insulin, 100 IU/mL penicillin, and 100 μg/mL streptomycin.
417 The ATCC Madin-Darby canine kidney (MDCK) cells used in the viral entry inhibition

assay were grown in Dulbecco's modified Eagle's medium (Gibco BRL Inc., Gaithersburg, MD, USA) and cultured with similar supplements as those of the cancer cells. All abovementioned cells were maintained in a humidified incubator at 37 °C and 5% CO_2.

4.7. Luminescent cell viability assay

The treatment effects of compounds **1**, **2**, **4**, and 5-fluorouracil (positive control) on cell proliferation were determined using the CellTiter-Glo® Luminescent Cell Viability Assay (Promega, Madison, WI, USA). All compounds were prepared in 100 mM DMSO as a stock solution and diluted to various concentrations (1.65 to 100 μM) using sterile phosphate buffer saline. Cancerous and non-cancerous cells were seeded in 384-well opaque plates for 24 h at a density of 1000 cells/well, followed by treatment with **1**, **2**, **4**, and 5-fluorouracil for 72 h. Cells treated with 0.1% DMSO were used as negative controls. Luminescence reading was measured using SpectraMax M3 Multi-Mode microplate reader (Radnor, USA). The half-maximal inhibitory concentration (IC_{50}) was determined based on the percentage cell viability calculated from the luminescent reading of treated cells and cells treated with the negative control. Statistical significance between the tested compounds and 5-fluorouracil (a clinically used chemotherapy agent) was performed using one-way analysis of variance (ANOVA) *post hoc* Dunnett's *t*-test via SPSS (version 18.0). Results were considered statistically significant if p-value < 0.05.

4.8. Viral entry inhibition assay

A pseudotyped virus was generated as described elsewhere (Scott et al., 2016) expressing the haemagglutinin (HA) of influenza strain A/Viet Nam/1194/2004 (H5N1), kindly provided by Dr Nigel Temperton (University of Kent, Medway School of Pharmacy). Equal volumes (50 μL) of compounds **4**, **5**, and **6** were individually incubated in triplicate at 10 μg/mL with the HA pseudotyped virus at 1 x 10^6 relative light units (RLU) per well for 1 hour at 37 °C. Next, 1 x 10^4 MDCK cells were added to each well. Controls such as virus-only (without compound) and cell-only (without virus and compound) were included. After incubation at 37 °C in 5% CO_2 for 48 hours, the cells were observed for cell growth before supernatant was removed and the cells lysed for 10 minutes with 50 μL of SteadyGlo reagent (Promega, Madison, WI, USA). Luminescence reading (RLU) was measured using an Orion L Microplate Luminometer

(Titertek-Berthold, Germany). The percentage (%) inhibition caused by the compounds relative to the virus-only control was calculated based on the below formula:

$$\frac{\text{Virus control only RLU} - \text{Compound and virus RLU}}{\text{Virus control only RLU}} \times 100\%$$

Declaration of competing interest

The authors declare that they have no known competing financial interests or personal relationships that could have appeared to influence the work reported in this paper.

Acknowledgments

This research did not receive any specific grant from funding agencies in the public, commercial, or not-for-profit sectors.

Appendix A. Supplementary data

Supplementary data related to this article can be found at

Captions for Figures:

Fig. 1. Structures of compounds **1**–**8**.

Fig. 2. ^{1}H–^{1}H COSY and selected HMBC correlations of compounds **1**–**4**.

Fig. 3. Selected NOESY correlations of compounds **1**–**3**.

Fig. 4. X-ray crystal structure of compound **1**.

Fig. 5. Plausible biosynthetic pathway to compounds **1** and **2** from cucurbitacin F (**9**).

Fig. 6. Viral entry inhibition assay using influenza HA pseudotyped virus showing (a) the mean and standard deviation of relative light units (RLU) per ml (triplicate wells from a representative assay) caused by compounds **4**–**6** relative to the virus-only control (shown by dotted line); and (b) the calculated mean percentage inhibition relative to the virus-only control.

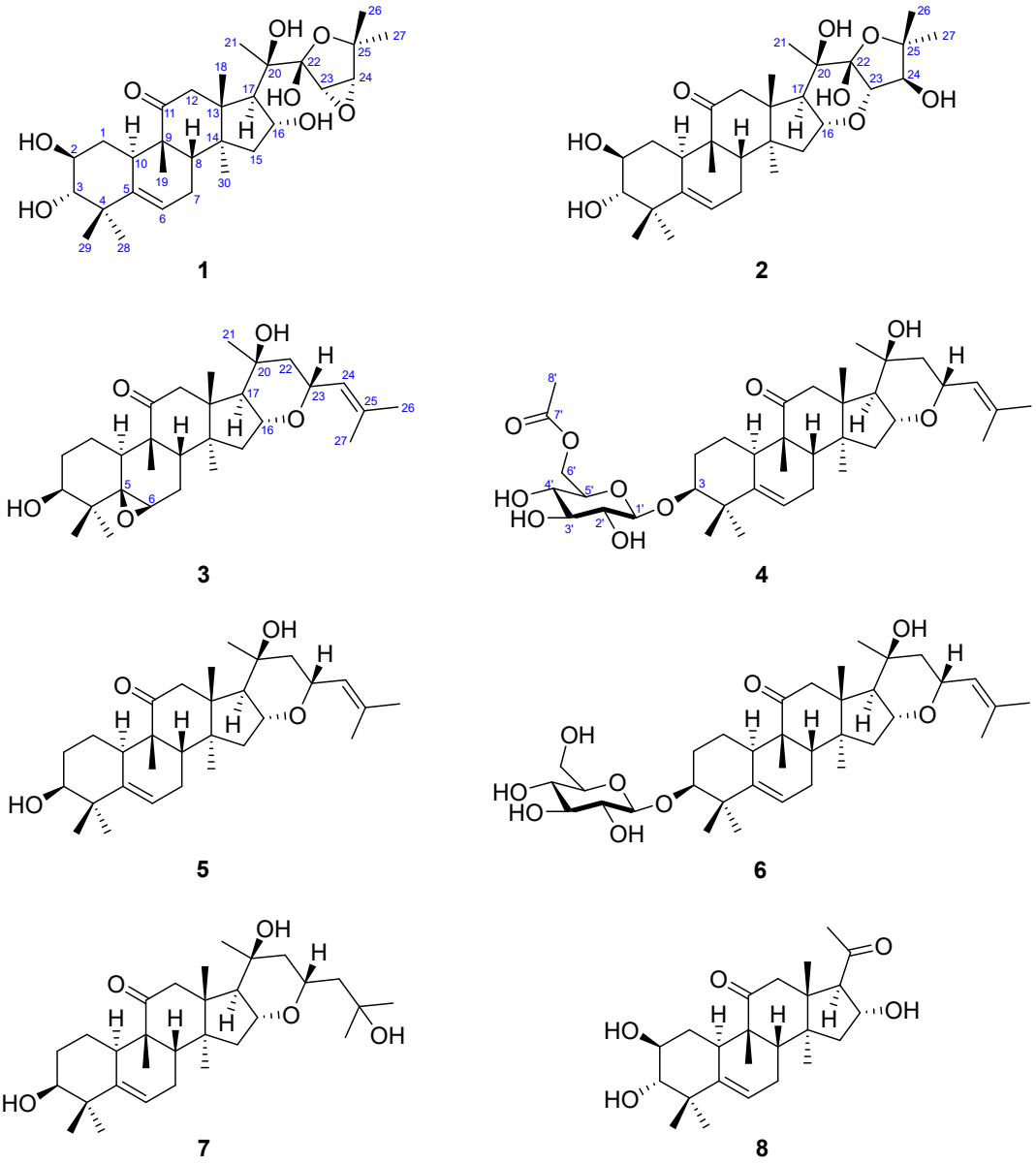

Fig. 1.

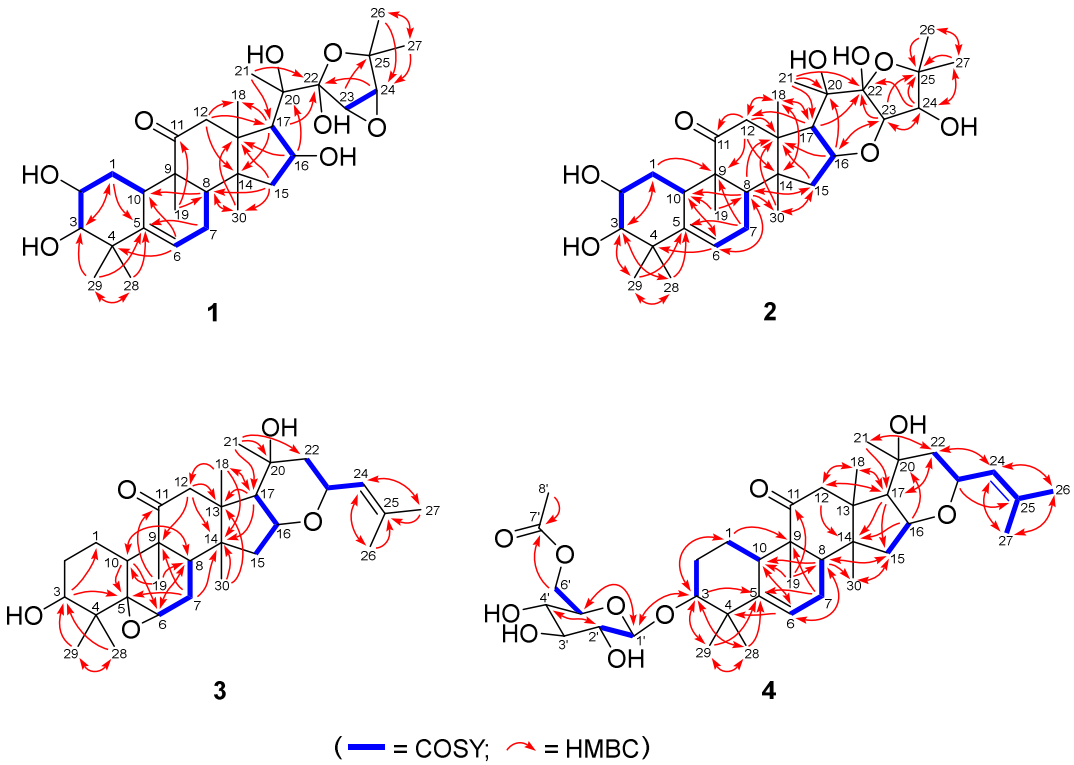

Fig. 2.

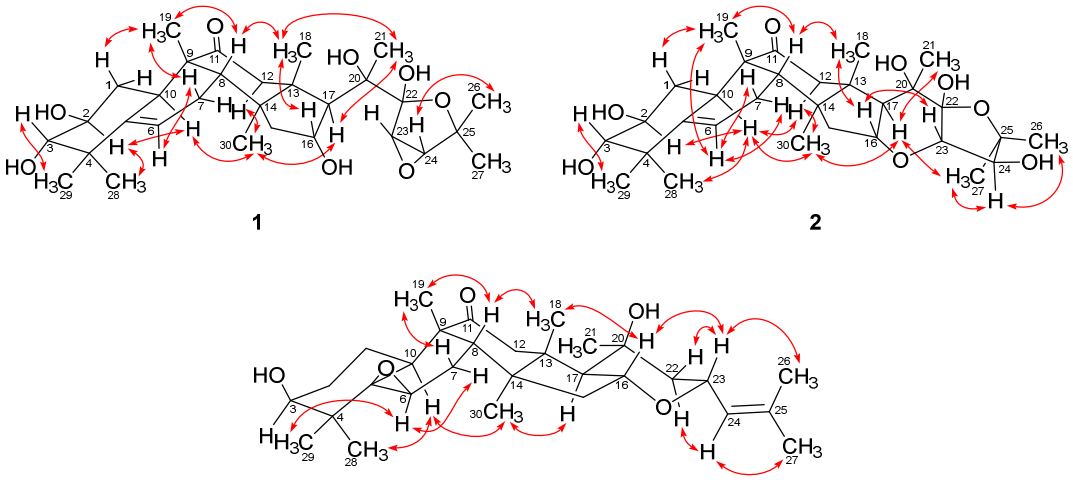

Fig. 3.

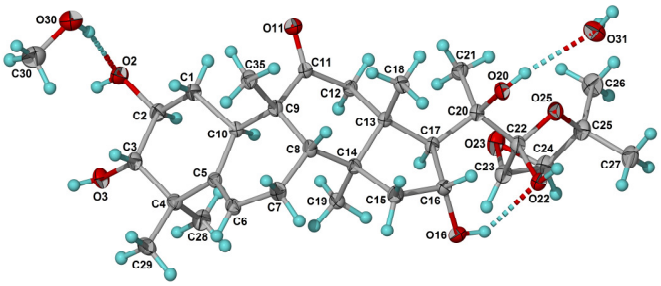
O30
O11
O31
O2
C30
C1
C35
C11
C18
C21
C26
C12
O20
O25
C2
C9
C13
C20
C22
C25
C10
C17
O23
C24
C3
C8
C14
C23
C27
C5
O3
C4
C7
C19
C15
C16
O22
C6
C28
O16
C29

Fig. 4.

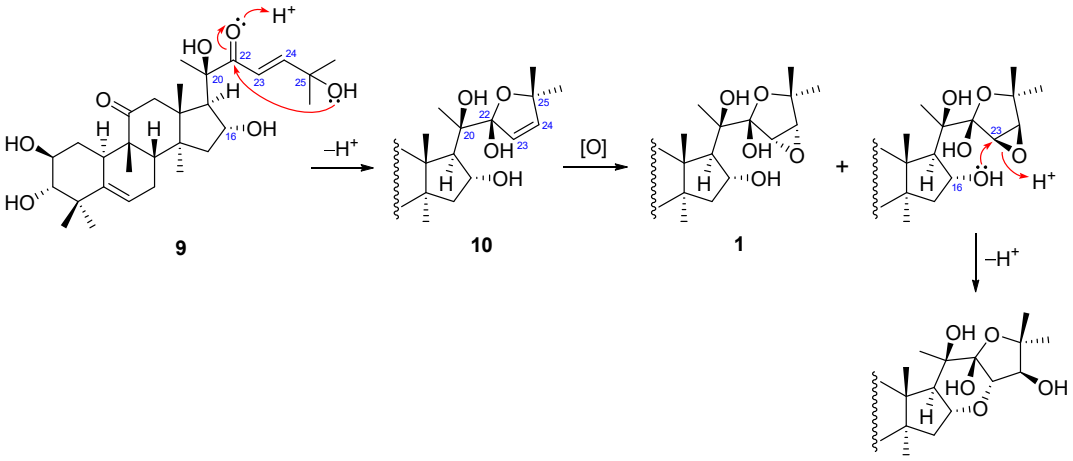
H+
HO
O
22
24
20
23
25
OH
H
O
H
H
HO
HO
16
OH
9
–H+
OH
O
25
22
24
20
OH
23
H
OH
10
[O]
OH
O
OH
O
H
OH
1
+
OH
O
23
HO
O
H
16
OH
H+
–H+
OH
O
HO
OH
H
O
2

Fig. 5.

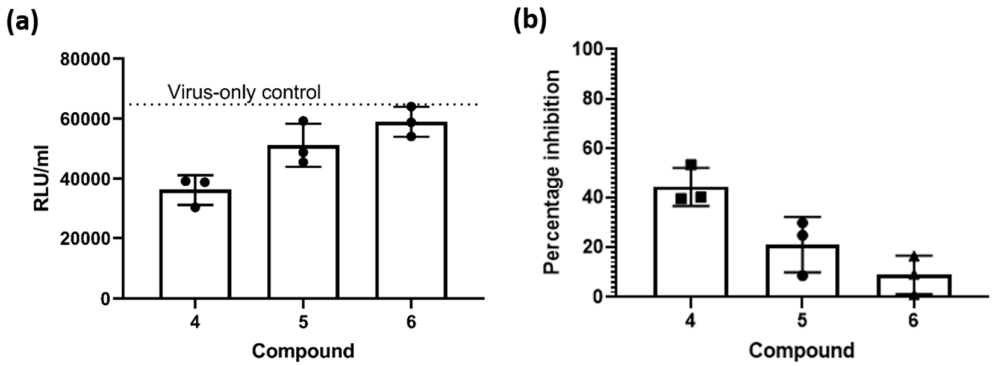
(a)
80000
60000
40000
20000
0
RLU/ml
Virus-only control
4
5
6
Compound
(b)
100
80
60
40
20
0
Percentage inhibition
4
5
6
Compound

Fig. 6.

Table 1. ^{1}H and ^{13}C NMR spectroscopic data for **1** and **2** (600 MHz, $CDCl_3$)[a].

Position	**1**		**2**	
	δ_H (mult., *J* in Hz)	δ_C	δ_H (mult., *J* in Hz)	δ_C
1	1.08, m	33.3	1.08, m	33.1
	1.87, m		1.86, m	
2	3.57, ddd (11.3, 9.3, 4.2)	71.0	3.54, m	70.8
3	2.97, d (9.3)	80.9	2.93, d (9.1)	80.7
4		41.9		41.9
5		140.6		140.9
6	5.73, d (5.8)	119.2	5.71, d (5.9)	119.0
7α	1.97, dd (18.3, 6.1)	23.8	1.92, dd (18.7, 6.1)	23.8
7β	2.38, m		2.39, m	
8	1.92, d (8.1)	42.5	1.96, d (7.9)	42.6
9		48.2		48.8
10	2.33, d (12.9)	33.9	2.28, m	33.7
11		213.7		213.7
12α	3.11, d (14.6)	49.2	3.02 d (14.8)	48.0
12β	2.65, d (14.6)		2.44 d (14.8)	
13		47.6		48.9
14		51.8		47.7
15α	1.53, d (13)	44.3	1.40, dd (13, 3.5)	40.3
15β	1.87, dd (13, 8.4)		1.82, dd (13, 10)	
16	4.60, dd (8.4, 6.7)	71.2	4.47, td (10, 3.2)	75.4
17	2.42, d (6.5)	56.6	2.42, d (9)	50.4
18	0.94, s	19.3	0.927, s	19.8
19	1.08, s	20.2	1.09, s	20.7
20		77.4		74.3
21	1.50, s	24.6	1.26, s	20.3
22		106.3		105.2
23	3.84, d (2.8)	59.6	4.04, br s	86.9
24	3.47, d (2.8)	59.7	3.82, br s	80.4
25		81.2		87.0
26	1.34, s	23.0	1.36, s	25.0
27	1.39, s	25.3	1.38, s	28.6
28	0.94, s	21.6	0.934, s	21.5
29	1.19, s	24.7	1.18, s	24.6
30	1.27, s	18.8	1.19, s	20.3

[a] Assignments based on the COSY, HSQC, and HMBC spectra.

Table 2. ^{1}H and ^{13}C NMR spectroscopic data for **3** and **4** (600 MHz, $CDCl_3$)[a].

Position	**3**		**4**	
	δ_H (mult., *J* in Hz)	δ_C	δ_H (mult., *J* in Hz)	δ_C
1	0.92, m	19.6	1.35, m	21.1
	1.52, m		1.53, m	
2	1.78, m	29.6	1.66, m	27.7
	1.78, m		1.91, m	
3	3.47, br s	77.8	3.35, m	86.7
4		39.7		41.4
5		65.4		140.3
6	3.26, d (5.6)	52.2	5.57, d (5.6)	118.6
7α	1.82, m	22.5	1.85, m	23.8
7β	2.25, dd (16.4, 8.9)		2.38, m	
8	1.86, d (8.7)	41.6	1.93, m	42.7
9		48.0		49.4
10	2.16, m	32.7	2.22, m	35.3
11		212.8		213.8
12α	2.99, d (14.7)	48.3	3.01, d (14.6)	48.3
12β	2.44, d (14.7)		2.42, d (14.6)	
13		49.0		48.0
14		47.0		48.3
15α	1.52, m	40.8	1.47, m	40.7
15β	1.82, m		1.83, m	
16	4.37, td (10.2, 3.6)	75.9	4.36, td (10.2, 3.2)	76.2
17	1.91, d (10)	55.5	1.94, m	55.0
18	0.89, s	18.9	0.93, s	19.8
19	1.17, s	19.2	1.10, s	20.2
20		72.2		72.3
21	1.31, s	29.2	1.30, s	29.2
22α	1.45, m	49.0	1.44, m	49.0
22β	1.36, m		1.37, m	
23	4.54, ddd (11.2, 8.3, 2.7)	72.9	4.53, ddd (11.2, 8.7, 2.6)	72.9
24	5.15, d (8.2)	125.0	5.14, d (8.4)	125.1
25		136.4		136.2
26	1.69, s	18.4	1.69, s	18.4
27	1.72, s	25.8	1.71, s	25.8
28	1.10, s	24.7	1.00, s	27.5
29	0.91, s	20.4	1.18, s	25.5
30	1.27, s	22.9	1.21, s	21.0
1'			4.24, d (7.8)	104.2
2'			3.40, m	74.0
3'			3.50, m	76.1
4'			3.35, m	70.3
5'			3.40, m	73.6
6'			4.30, m	63.5
7'				171.6
8'			2.09, s	20.9

[a] Assignments based on the COSY, HSQC, and HMBC spectra.

625 **Table 3.** Cytotoxic activities of **1**, **2**, and **4** against a panel of human cancer cell lines.

Compounds	$IC_{50} \pm SD$ (μM)										
	MDA-MB-468[a]	MDA-MB-231[a]	MCF-7[a]	SKBR3[a]	AsPC-1[b]	BxPC-3[b]	SW1990[b]	SW48[c]	Caco2[c]	HCT116[c]	MCF-10A[d]
1	7.4 ± 1.5*	9.2 ± 1.0*	9.3 ± 1.8*	10.6 ± 3.2*	17.6 ± 1.3	23.8 ± 3.6*	28.58 ± 3.7*	4.6 ± 0.5*	61.8 ± 4.2*	92.8 ± 6.9*	49.7 ± 2.7
2	10.5 ± 1.7*	10.7 ± 1.4*	19.0 ± 4.3	23.6 ± 2.5	11.6 ± 0.5	23.0 ± 1.8	33.58 ± 2.7	ND	ND	ND	35.0 ± 1.2
4	10.7 ± 1.6*	15.3 ± 0.5*	22.2 ± 2.9	33.9 ± 3.9	43.1 ± 5.2	>100	42.1 ± 1.3	ND	ND	ND	41.9 ± 8.4
5-fluorouracil (positive control)	70.6 ± 4.7	79.9 ± 2.1	23.9 ± 0.5	25.4 ± 5.7	35.2 ± 0.7	52.7 ± 1.1	45.4 ± 2.3	24.4 ± 1.3	35.4 ± 0.7	37.91 ± 0.2	44.6 ± 6.4

626 [a] Human breast adenocarcinoma.

627 [b] Human pancreatic adenocarcinoma.

628 [c] Human colorectal adenocarcinoma.

629 [d] Non-tumorigenic breast epithelial cell line.

630 ND = Not determined.

631 * Statistically significantly different from 5-fluorouracil ($p < 0.05$).

References

Aggarwal, S. 2001. *Elaeocarpus* L., in: van Valkenburg, J.L.C.H., Bunyapraphatsara, N. (Eds), Plant Resources of South-East Asia No. 12(2): Medicinal and poisonous plants 2. Backhuys Publishers, Leiden, The Netherlands, pp. 241–246.

Cai, Y., Fang, X., He, C., Li, P., Xiao, F., Wang, Y., Chen, M., 2015. Cucurbitacins: A systematic review of the phytochemistry and anticancer activity. Am. J. Chin. Med. 43, 1–20. https://doi.org/10.1142/S0192415X15500755

Chan, Z.-Y., Krishnan, P., Moderasi, S.M., Hii, L.-W., Mai, C.-W., Lim, W.-M., Leong, C.-O., Low, Y.-Y., Wong, S.-K., Yong, K.-T., Leong, A.Z.-X., Lee, M.-K., Ting, K.-N., Lim, K.-H., 2021. Monomeric, dimeric, and trimeric tropane alkaloids from *Pellacalyx saccardianus*. J. Nat. Prod. 84, 2272–2281. https://doi.org/10.1021/acs.jnatprod.1c00374

Che, C.-T., Fang, X., Phoebe Jr., C.H., Kinghorn, A.D., Farnsworth, N.R., Yellin, B., Hecht, S.M., 1985. High-field ^{1}H-NMR spectral analysis of some cucurbitacins. J. Nat. Prod. 48, 429–434. https://doi.org/10.1021/np50039a010

Chen, J.C., Chiu, M.H., Nie, R.L., Cordell, G.A., Qiu, S.X., 2005. Cucurbitacins and cucurbitane glycosides: structures and biological activities. Nat. Prod. Rep. 22, 386–399. https://doi.org/10.1039/B418841C

Donders, L.A., de Leeuw, F.A.A.M., Altona, C., 1989. Relationship between proton-proton NMR coupling constants and substituent electronegativities IV. An extended Karplus equation accounting for interactions between substituents and its application to coupling constant data calculated by the extended Huckel method. Magn. Reson. Chem. 27, 556–563. https://doi.org/10.1002/mrc.1260270608

Ezeoke, M.C., Krishnan, P., Sim, D.S.-Y., Lim, S.-H., Low, Y.-Y., Chong, K.-W., Lim, K.-H., 2018. Unusual phenethylamine-containing alkaloids from *Elaeocarpus tectorius*. Phytochemistry 146, 75–81. https://doi.org/10.1016/j.phytochem.2017.12.003

Fang, X., Phoebe Jr., C.H., Pezzuto, J.M., Fong, H.H.S., Farnsworth, N.R., 1984. Plant anticancer agents, XXXIV. Cucurbitacins from *Eleaocarpus dolichostylus*. J. Nat. Prod. 47, 988–993. https://doi.org/10.1021/np50036a013

Haasnoot, C.A.G., de Leeuw, F.A.A.M., Altona, C., 1980. The relationship between proton-proton NMR coupling constants and substituent electronegativities—I: An empirical generalization of the Karplus equation. Tetrahedron 36, 2783–2792.

https://doi.org/10.1016/0040-4020(80)80155-4

Hüttel, W., Spencer, J.B., Leadlay, P.F., 2014. Intermediates in monensin biosynthesis: A late step in biosynthesis of the polyether ionophore monensin is crucial for the integrity of cation binding. Beilstein J. Org. Chem. 10, 361–368. https://doi.org/10.3762/bjoc.10.34

Little, R.F., Samborskyy, M., Leadlay, P.F., 2020. The biosynthetic pathway to tetromadurin (SF2487/A80577), a polyether tetronate antibiotic. PLoS ONE 15, e0239054. https://doi.org/10.1371/journal.pone.0239054

Ito, A., Chai, H.-B., Lee, D., Kardono, L.B.S., Riswan, S., Farnsworth, N.R., Cordell, G.A., Pezzuto, J.M., Kinghorn, A.D., 2002. Ellagic acid derivatives and cytotoxic cucurbitacins from *Elaeocarpus mastersii*. Phytochemistry 61, 171–174. https://doi.org/10.1016/S0031-9422(02)00232-7

Kim, D.K., Choi, S.H., Lee, J.O., Ryu, S.Y., Park, D.K., Shin, D.H., Jung, J.H., Pyo, S.K., Lee, K.R., Zee, O.P., 1997. Cytotoxic constituents of *Sorbaria sorbifolia* var. *stellipila*. Arch. Pharm. Res. 20, 85–87. https://doi.org/10.1007/BF02974048

Krishnan, P., Lee, F.-K., Yap, V.A., Low, Y.-Y., Kam, T.-S., Yong, K.-T., Ting, K.-N., Lim, K-H., 2020. Schwarzinicines A–G, 1,4-diarylbutanoid–phenethylamine conjugates from the leaves of *Ficus schwarzii*. J. Nat. Prod. 83, 152–158. https://doi.org/10.1021/acs.jnatprod.9b01160

Kubo, H., Ohtani, K., Kasai, R., Yamasaki, K., Nie, R.-L., Tanaka, O., 1996. Cucurbitane glycosides from *Hemsleya panacis-scandens* rhizomes. Phytochemistry 41, 1169–1174. https://doi.org/10.1016/0031-9422(95)00722-9

Kwon, O.-K., Ahn, K.-S., Park, J.-W., Jang, H.-Y., Joung, H., Lee, H.-K., Oh, S.-R., 2012. Ethanol extract of *Elaeocarpus petiolatus* inhibits lipopolysaccharide-induced inflammation in macrophage cells. Inflammation 35, 535–544. https://doi.org/10.1007/s10753-011-9343-3

Meng, D., Qiang, S., Lou, L., Zhao, W., 2008. Cytotoxic cucurbitane-type triterpenoids from *Elaeocarpus hainanensis*. Planta Med. 74, 1741–1744. https://doi.org/10.1055/s-2008-1081356

Muñoz, O., Delporte, C., Backhouse, N., Erazo, S., Negrete, R., Maldonadob, S., López-Pérez, J.L., Feliciano, A.S., 2000. A New Cucurbitacin Glycoside from *Kageneckia oblonga* (Rosaceae). Z. Naturforsch. 55c, 141–145. https://doi.org/10.1515/znc-2000-3-403

Pan, L., Yong, Y., Deng, Y., Lantvit, D.D., Ninh, T.N., Chai, H., Carcache de Blanco,

E.J., Soejarto, D.D., Swanson, S.M., Kinghorn, A.D., 2012. Isolation, structure elucidation, and biological evaluation of 16,23-epoxycucurbitacin constituents from *Eleaocarpus chinensis*. J. Nat. Prod. 75, 444–452. https://doi.org/10.1021/np200879p

Quattrocchi, U. 2012. CRC World Dictionary of Medicinal and Poisonous Plants: Common Names, Scientific Names, Eponyms, Synonyms, and Etymology. CRC Press, Boca Raton, Florida.

Scott, S.D., Kinsley, R., Temperton, N., Daly, J.M., 2016. The optimisation of pseudotyped viruses for the characterisation of immune responses to equine influenza virus. Pathogens 5, 68. https://doi.org/10.3390/pathogens5040068

Si, L., Meng, K., Tian, Z., Sun, J., Li, H., Zhang, Z., Soloveva, V., Li, H., Fu, G., Xia, Q., Xiao, S., Zhang, L., Zhou, D., 2018. Triterpenoids manipulate a broad range of virus-host fusion via wrapping the HR2 domain prevalent in viral envelopes. Sci. Adv. 4, eaau8408. https://doi.org/10.1126/sciadv.aau8408

Tang, Y., Phengklai, C. 2007. Elaeocarpaceae, in: Wu, Z.Y., Raven, P.H., Hong, D.Y. (Eds), Flora of China, vol. 12. Science Press and Missouri Botanical Garden Press, Beijing, St. Louis, pp. 223–239.

Turner, A., Bond, D.R., Vuong, Q.V., Chalmers, A., Beckett, E.L., Weidenhofer, J., Scarlett., C.J., 2020. *Elaeocarpus reticulatus* fruit extracts reduce viability and induce apoptosis in pancreatic cancer cells *in vitro*. Mo. Biol. Rep. 47, 2073–2084. https://doi.org/10.1007/s11033-020-05307-8

Ye, M., Liao, Y., Wu, L., Qi, W., Choudhry, N., Liu, Y., Chen, W., Song, G., Chen, J., 2020. An oleanolic acid derivative inhibits hemagglutinin-mediated entry of influenza A virus. Viruses 12, 225. https://doi.org/10.3390/v12020225

Zhang, S., Tao, Z.-M., Zhang, Y., Shen, Z.-W., Qin, G.-W., 2010. Chemical Constituents from the sems and leaves of *Elaeocarpus glabripetalus*. Chin. J. Nat. Med. 8, 21–24. https://doi.org/10.1080/14786419.2019.1637870